

Detection of single and multiple IGBTs open-circuit faults in a field-oriented controlled induction motor drive

PIOTR SOBAŃSKI, TERESA ORŁOWSKA-KOWALSKA

*Department of Electrical Machines, Drives and Measurements
Wrocław University of Science and Technology
Wybrzeże Wyspiańskiego 27, 50-370 Wrocław
e-mail: {piotr.sobanski/teresa.orlowska-kowalska}@pwr.edu.pl*

(Received: DD.MM.YEAR, revised: DD.MM.YEAR)

Abstract: In this paper a transistor open-circuit fault diagnosis method in a rotor field oriented controlled induction motor drive, fed by a two-level voltage inverter has been proposed. The diagnostic procedure ensures detection and localization of single or multiple power switch failures in time shorter than one period of a stator current fundamental harmonic, without regard to a drive operation point. A new simple scheme of the diagnostic system is proposed. In order to validate the proposed transistor fault diagnostic method, a detailed simulation as well as experimental tests of the field-oriented control drive system were carried out and some of them are shown in this paper.

Key words: induction motor; field-oriented control; condition monitoring; open-circuit fault; fault diagnosis

1. Introduction

Induction motors (IM) are the most popular electrical machines in industry nowadays because of their robust construction and relatively low manufacturing cost. They are practically maintenance-free and they assure very good dynamic performance if appropriate control structure is applied. The aforementioned qualities have been researched and improved by using intelligent and sophisticated control methods based on the field oriented control (FOC) or the direct torque control (DTC) because these control concepts enable both the amplitude and phase control of ac-excitation. In general, these adjustable IM drives are composed of advanced structures that include the static inverter, induction motor, control blocks, electrical and mechanical connections, sensors, etc. Thus, the total reliability of the drive system can be improved by increasing the reliability of each single component or by decreasing the number of the structure components of a drive through the development of sensorless drives [1, 2].

Faults of power electronics, an electrical motor or sensors in adjustable-speed electrical motor drives can significantly disturb the control process, resulting in a drive availability

decrease. As a result, in the last decades, the interest of many members of the drives community and marketplace has been focused on new control techniques, that allow simultaneous electric drive operation after faults occurrence [3]. These techniques, known as fault-tolerant control (FTC) methods, integrate failure diagnosis algorithms and hardware or software redundancy that allow correct drive operation under its faulty condition. In [4] motor speed sensor fault-tolerant control technique based on the drive angular speed estimation is presented. The speed sensor failure is detected by analysing the error between the measured and estimated motor speed. According to this method, if a sensor is faulty, the drive operates using the estimated signal for the speed control. In [5] the hardware redundancy is utilized for the current sensor fault-tolerant control. The faulty sensor is replaced with the healthy ones. In the case of transistor failures the redundant converter topologies are required [6, 7]. First, the faulty transistor is isolated and then, thanks to the converter circuit reconfigurations, the post-fault control is implemented. The effectiveness of faults diagnostic techniques, namely correct failure detection and its localization, robustness against false alarms as well as fast diagnosis have an important influence on the possibility of an appropriate remedial action.

Among various types of faults, power converter faults, related to semiconductor or control circuit damages, are the most frequent ones and are estimated to make up to 60% of power device failures [8]. Thus recently quite a lot of different fault detection and localization methods and techniques devoted to power converters have been reported in technical literature. Surveys of diagnostic methods dedicated to transistor failures are presented in many works, e.g. [9]. In fact, they are hardware- and software-based transistor faults diagnostic techniques. The most frequently used approaches are based on the analysis of easily accessible signals, such as measured current or estimated voltage, thus these methods are usually classified as current- or voltage-based ones. It is important that, in accordance with these techniques, no additional measurement systems are utilized, in most cases. Many transistor failure monitoring techniques are based on the analysis of standardized errors between the reference estimated, predicted or measured variables [10-15]. For this purpose, the average values of these errors, which are additionally normalized by dividing them by the module of the variable vector, are calculated. Thanks to signal normalization the constant fault threshold can be assumed. The effectiveness of some of these techniques depends on the accuracy of the used estimation or prediction algorithms. Moreover, they require a relatively high computational effort so the industrial application of these algorithms is limited.

The second group of the transistor fault diagnostic methods consists of techniques based on the analysis of vector hodographs of the fault diagnostic variables [16-19]. A vast majority of these algorithms use the current vector whose amplitude is load-dependent. To overcome this disadvantage the flux vector, whose amplitude is stabilized for speed control, is utilized [16].

Unfortunately, some of the diagnostic methods are applied by using sophisticated algorithms, such as fuzzy-logic techniques [16] or neural networks [20, 21], that require a relatively high computational effort, so their applications are limited.

In this paper, an open-circuit fault diagnostic method for transistors with a two-level voltage inverter is developed and extensively tested. The technique is dedicated to vector-controlled AC-drives fed by a two-level inverter with the voltage Space Vector Modulation

(SVM). The diagnostic procedure ensures the detection and localization of single power switch failures as well as single-phase transistor faults, in time shorter than one period of the stator current fundamental harmonic, without regard to a drive operation point. In order to reduce an implementation effort of the solution, a scheme of the diagnostic system was simplified compared to the solution presented by the authors in previous work [17, 18]. In comparison to the methods described in the introduction, the developed algorithm is simpler to implement, which improves its applicability, in particular in the case of the low cost motor drive systems. Additionally, the method was validated by simulation and experimental tests, in different operation conditions of the drive system. The tests were carried out in the direct rotor field oriented controlled (DRFOC) induction motor drive under single and multiple switch open-circuit failures. To prove the diagnostic method robustness against false alarms simulation as well as experimental tests under various healthy motor drive operations have been carried out. The presented method was validated not only during constant speed and load of the drive but also under the drive acceleration and deceleration as well as rapid load changes.

2. Description of the fault diagnosis method

In Fig. 1a, the basic scheme of two-level voltage source inverter topology, whose faults are considered in this paper, is presented. For this inverter only eight switch-status combinations are possible, so that eight voltage vectors described as U_0, \dots, U_7 can be generated, according to Fig. 1b. In accordance with the diagnostic algorithm, detection and localization of transistor faults can be carried out by processing signals related to reference inverter voltages, generated in the control structure of the drive system, based on the rotor-field-oriented control (DRFOC), as it is presented in Fig. 1c.

These voltages can be produced by using eight combinations of the switch status. In order to achieve a reference voltage vector U_r , whose position in the α - β plane is defined by an angle γ , that is referred to the α axis, six active voltage vectors (U_1, \dots, U_6) and two zero ones (U_0 and U_7) are used. These vectors divide the α - β plane into six sectors: I, ... , VI, in accordance with (1):

$$SN = \text{int}\left(\frac{\gamma}{\pi/3}\right) + 1, \quad (1)$$

where int means the operation that returns the integer value.

Extraction of fault information is based on monitoring the voltage vector presence time t_M in the specific sectors of the complex α - β plane. Depending on motor speed direction and fault location, in a drive steady state, the reference voltage vector is forced in one characteristic sector during a much longer time-period than in the case of some other ones [16]. The direction of the voltage vector rotation is related to the angular motor speed direction. In further considerations it was assumed that under the motor mode of the machine, which rotates in the positive speed direction, the voltage space vector rotates in the positive direction as well. This means that the numbers of the sectors are increasingly changed.

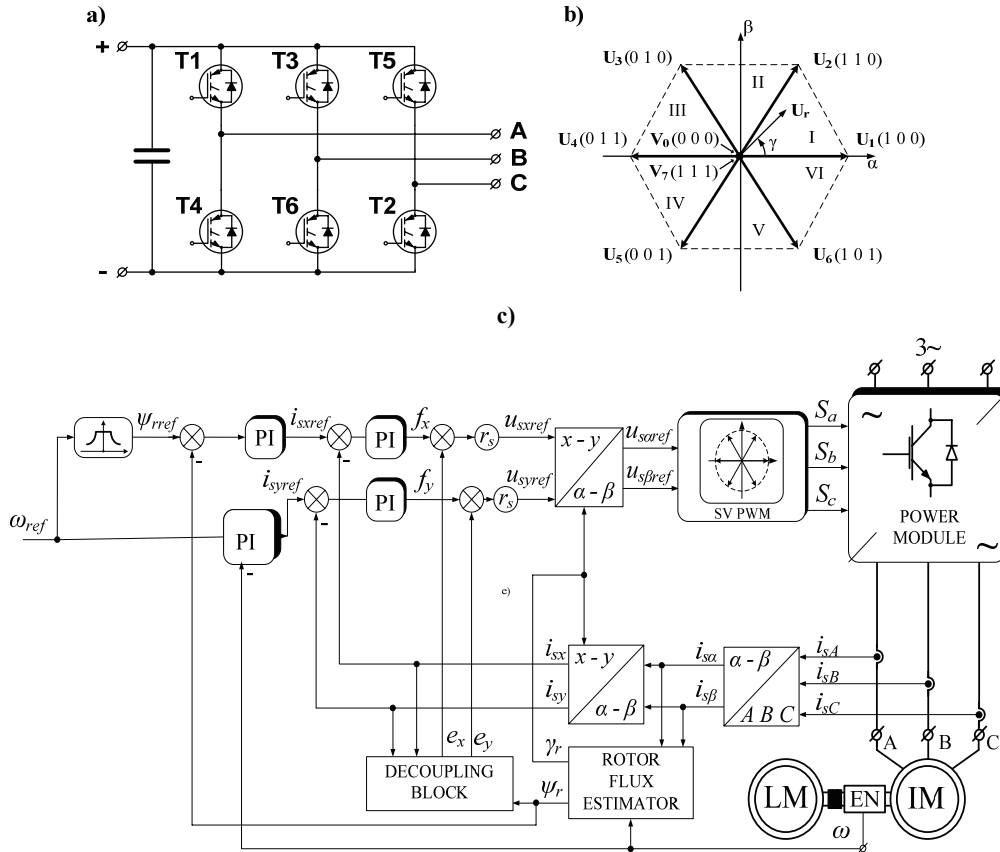


Fig. 1. A standard three-phase voltage source inverter: topology (a), voltage space vectors (b), DRFOC structure (c)

In this paper, a new simple implementation scheme of the diagnostic method described in detail in [17] is proposed, namely a number of counters used to realize the diagnostic system has been decreased from six to one. Additionally, to localize the faulted transistor, the signal SN is considered in the rule base. The block diagram of the analysed transistor fault diagnostic system is shown in Fig. 2.

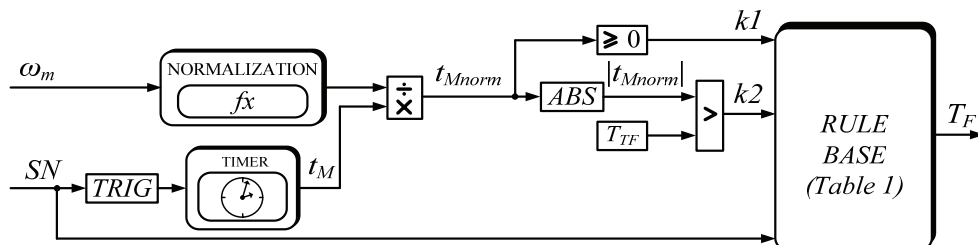


Fig. 2. A block diagram of the transistor faults diagnostic system

In this system, the counter whose frequency is equal to 5 kHz is activated by a triggering event, which consists in a change of the sector SN that describes the position of the reference voltage vector on the α - β plane. The value of the output counter signal t_M is proportional to the duration when the reference voltage vector is located in particular sectors. Due to the fact that the voltage frequency changes depending on the required motor speed, the diagnostic variable t_M is normalized by assuming the linear relationship between the speed and the reference voltage resulting in (2):

$$t_{M\text{norm}} = 6nt_M / (f_{\text{Timer}}T_Nn_N), \quad (2)$$

where n is the drive speed, f_{Timer} means the timer frequency, T_N is the period of the nominal voltage and n_N means the nominal speed, number 6 appears in the nominator of (2), because the α - β plane is divided into 6 sectors. Thanks to the normalization, for the healthy motor drive operations, a constant maximum value of the diagnostic signal $|t_{M\text{norm}}| = 1$ is obtained. If the signal $|t_{M\text{norm}}|$ reaches the fault threshold T_{TF} , then the transistor fault is detected. In order to localize a faulty switch, the rule base which considers the motor speed direction is utilized in accordance with Table 1. Logical variables $k1$ and $k2$ are related to the comparators of the diagnostic system (see Fig. 2).

Table 1. Open-switch fault symptoms patterns

Faulted switch T_F	$k1$	$k2$	SN
$T1$	1	1	1
	0	1	6
$T2$	1	1	2
	0	1	1
$T3$	1	1	3
	0	1	2
$T4$	1	1	4
	0	1	3
$T5$	1	1	5
	0	1	4
$T6$	1	1	6
	0	1	5

3. Simulation results of the IGBT fault detection method in a DRFOC-based induction motor drive

3.1. A short presentation of the simulation model and research scenario

This section presents selected simulation results which prove the effectiveness of the transistor fault diagnostic method. The presented results were obtained using a simulation model of the DRFOC induction motor drive system, which was using Matlab/Simulink and the specialized Sim Power Systems toolbox. In order to simulate open-switch faults, transistor gate control signals were removed, which results in non-conduction mode of the transistors. An assumed voltage modulation period is equal to 100 μ s similarly to the experimental research described in Section 4. The nominal parameters of the induction machine are shown in Table 2 in the Appendix.

The simulation results are presented according to the following scenario. First, the diagnostic method robustness against the false alarms during the healthy motor drive operations is validated. Then, the open-circuit transistor failures are studied under a constant reference angular speed ω_m and a different load torque m_l of the motor drive system, namely the algorithm was tested for the almost fully-loaded motor ($m_l = 0.8m_N$) under the fault of $T1$ then the load was rapidly decreased to $m_l = 0.2m_N$ and the switch failure of $T4$ was simulated. Moreover, the diagnostic algorithm was validated for the transistor faults occurring during motor speed accelerations and rapid (step) load changes. In figures, a magenta dotted line indicates the fault occurrence, but a moment of the fault detection is depicted as a blue or yellow dotted line. In order to rate the speed of the transistor failures diagnosis procedure, the normalized fault localization time t_{TF} is defined in accordance with (3):

$$t_{TF} = \frac{t_{\text{fault}}}{T_i}, \quad (3)$$

where t_{fault} means the time period between two instants: the fault occurrence and the fault localization, but T_i means the period of the current waveform which is measured shortly before the failure occurrence.

To prove the effectiveness of the considered transistor fault diagnostic method, transients of the diagnostic variable $|t_{M\text{norm}}|$ that are compared with the failure threshold T_{TF} , are presented. As proved in the next section of this paper, this threshold could be equal to 1.15, nevertheless in order to present the method more clearly, for the simulations it is assumed that $T_{TF} = 1.5$. Additionally, relevant transients of the signal SN referred to the number of the sector, which describe the position of the reference voltage vector in the α - β stationary coordinates system, are shown. Moreover, phase currents $i_{s,A,B,C}$, reference speed $\omega_{m\text{ref}}$ and the measured angular motor speed ω_m , are presented. The following results have a representative character and they are related to the transistor failures in phase A of the inverter. The observations for the faults in the phase B or C are analogical.

3.2. Validation of the diagnostic method robustness against false alarms

Taking into account healthy motor drive operations, the values of the diagnostic signal $|t_{M\text{norm}}|$ are less than one, so the fault threshold should be greater than one. To assume the appropriate value of this threshold, namely to avoid false alarms, the diagnostic system was tested during rapid (step) load changes from the nominal value to zero. Fig. 3 shows the time domain waveforms of the angular speed, currents, electromagnetic torque and diagnostic signal for healthy motor drive operations.

First, at the instant $t = 0.2$ s the motor was loaded when the drive was operating at a low speed. Then, at $t = 0.4$ s the load was changed from the nominal value to zero. Then, at $t = 0.5$ s the nominal load torque $m_l = m_N$ was applied (step change) once again and the speed was increased up to the nominal value. After that, at $t = 0.9$ s the load was suddenly reduced to zero. In Fig. 3e it is visible that the diagnostic signal does not exceed the assumed fault threshold not only during sudden load torque step changes but also during fast acceleration of the drive.

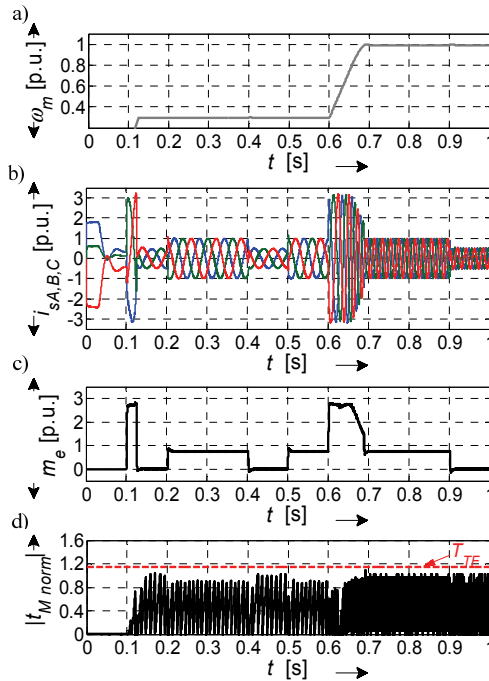


Fig. 3. Time domain waveforms achieved during the test of the diagnostic method robustness against false alarms ($T_{TF} = 1.15$) during a healthy mode

3.3. Validation of the diagnostic method under constant speed operation of the DRFOC drive

The LHS column of Fig. 4 presents simulation results achieved for the $T1$ failure, which occurred at the instant $t = 0.3$ s, under the transistor conducting mode.

In the LHS of Fig. 4 (c, d), it is visible that, for the $SN = 1$ at $t = 0.303$ s, the diagnostic signal achieved the fault threshold $T_{TF} = 1.5$, which is indicated by the green dotted line. For this case, the speed diagnosis takes 0.15 of the current fundamental period T_i . After that, at $t = 0.35$ s, the motor was loaded ($m_l = m_N$) and at the instant $t = 0.45$ s the fault of the lower transistor in phase A was simulated. As it can be seen in LHS of Fig. 4 (c, d) the failure of $T4$ was detected at $t = 0.47$ s, so the duration of the fault diagnosis was also shorter than one current fundamental period ($t_{TF} = 0.77$). Compared to the previously considered case, which illustrates the faulty drive operation under nominal motor speed, in the RHS of Fig. 4 faults of the inverter were simulated at the low velocity of the drive ($\omega_m = 0.4\omega_N$). When the $T1$ failure occurred the load torque was $m_l = 0.8m_N$, next, at the instant $t = 0.35$ s, the load was rapidly decreased to $m_l = 0.2m_N$. Then at $t = 0.45$ s the fault of $T4$ was simulated. The $T1$ failure was detected within the time that is equal to 0.35 of the current fundamental period but, in the case of $T4$ open-circuit failure the detection time was $t_{TF} = 0.98$ of T_i .

The simulation results show the effectiveness of the single and multiple transistor fault diagnostic method under various motor drive conditions, namely the changeable load and various motor speed that was referred as a constant values.

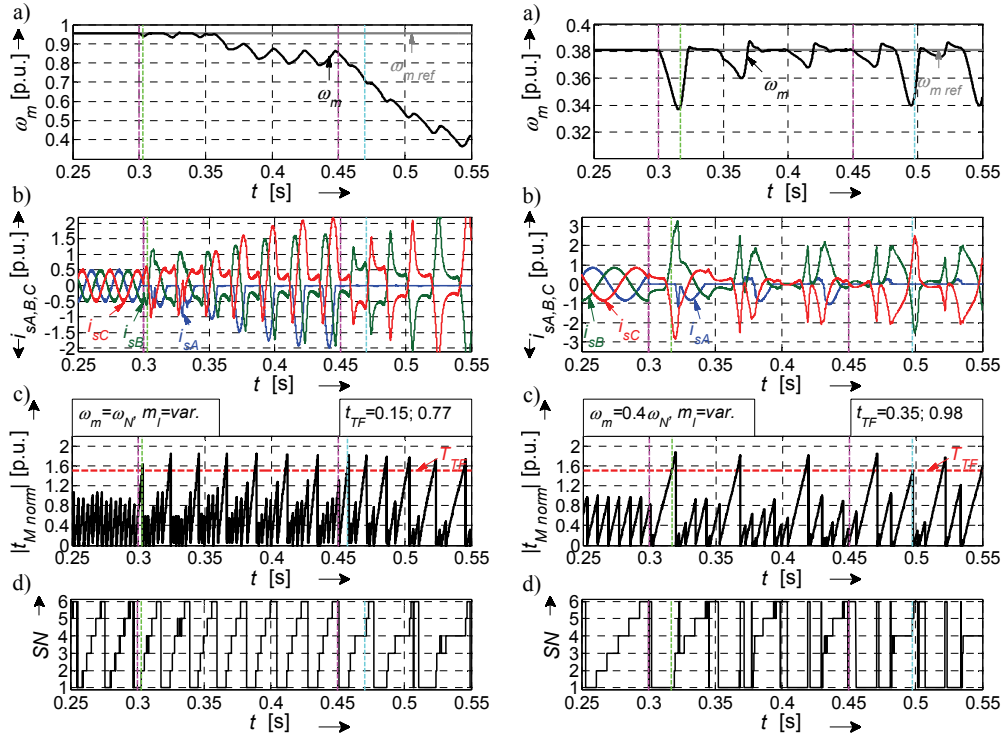


Fig. 4. Reference $\omega_{m\text{ref}}$ and measured ω_m angular motor speed (a), phase currents $i_{sA,B,C}$ (b), the diagnostic variable $|t_{M\text{norm}}|$ (c) and SN signal (d) for the motor drive operation under: LHS – nominal reference angular speed $\omega_{m\text{ref}} = \omega_N$, variable load torque and the fault of $T1$ and next $T4$; RHS – reference angular speed $\omega_{m\text{ref}} = 0.4\omega_N$, variable load torque and the fault of $T1$ and next $T4$

3.4. Evaluation of the diagnostic method under DRFOC drive operation with linear speed changes

Many electrical drives operate with frequent motor speed changes so it is necessary to validate also the effectiveness of the analysed fault diagnostic technique during speed acceleration and deceleration. The following part of the article shows simulation results that confirm the correctness of the diagnostic algorithm for the single as well as multiple transistor open-circuit faults occurring in the inverter phase (see Fig. 5).

In accordance with the presented tests, the fault of $T1$ transistor was simulated at $t = 0.30$ s, but the failure of $T4$ switch occurred at $t = 0.45$ s. Until $t = 0.35$ s the drive operated with the load $m_l = 0.8m_N$ and then was rapidly (step) changed to the value $m_l = 0.2m_N$. As shown in Fig. 5, the transistor fault diagnosis took less time than one current fundamental period. In accordance with the presented simulation results the transistor open-circuit fault diagnostic method is effective even when the drive operates at a linear speed and the rapid load changes as well. From Fig. 4 and Fig. 5 results, that the fault threshold can be taken lower than the assumed value in all operation condition of the drive system (see a remark in section 3.1), thus in the experimental tests this value was taken $T_{TF} = 1.15$.

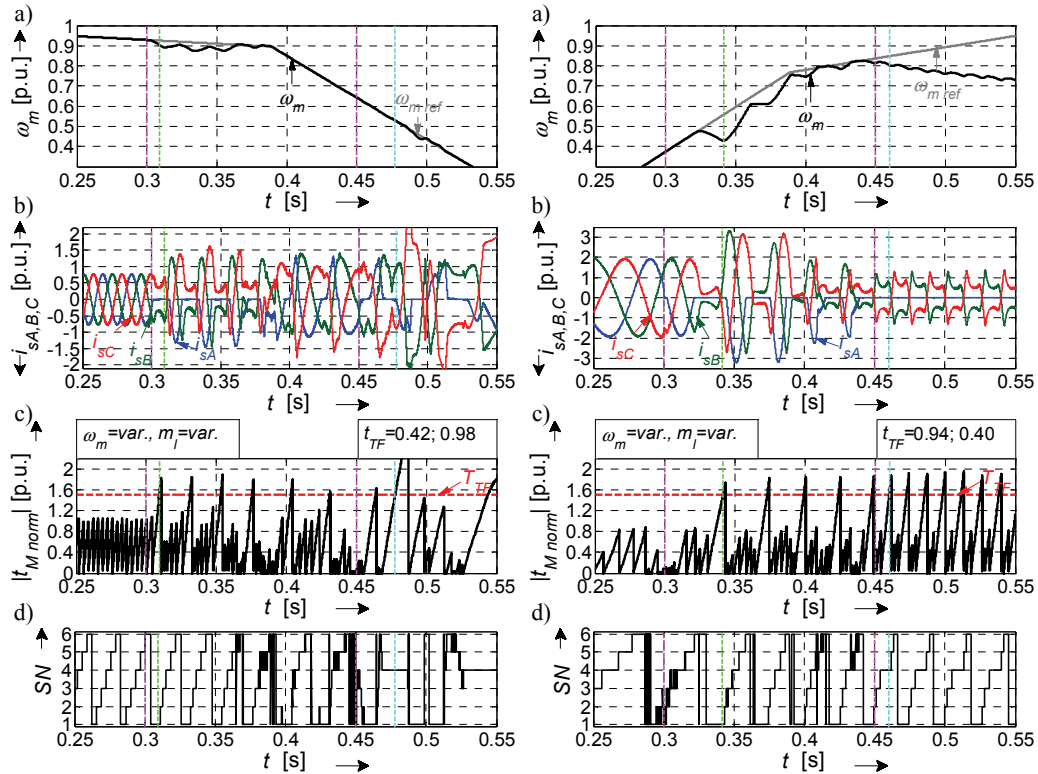


Fig. 5. Reference $\omega_{m,ref}$ and measured ω_m angular motor speed (a), phase currents $i_{sA, B, C}$ (b), the diagnostic variable $|t_{M, norm}|$ (c) and SN signal (d) for the motor drive operation under: LHS – speed acceleration; RHS – speed deceleration; variable load torque and the faults of $T1$ and next $T4$

4. Experimental validation of the IGBT fault detection method in a DRFOC-based induction motor drive

4.1. A short presentation of the experimental set-up and research scenario

In this section, selected experimental results, that confirm the effectiveness of the proposed open-switch fault diagnostic method, are presented. The research was carried out using a laboratory set-up whose schematic diagram and a picture are shown in Fig. 6 (for the same IM that was used in simulation tests). The experimental results, that are presented in this section, are organized in accordance with the following scenario. First, the diagnostic method robustness against the false alarms is tested. For this purpose the diagnostic signal $|t_{M, norm}|$ is analysed during the speed acceleration or its deceleration as well as rapid load changes. Then, the open-switch faults are obtained under a constant angular speed ω_m of the drive system. Next, the diagnostic method is tested for the failures that occur during motor speed acceleration. The results of the research have been presented similarly to the previously discussed simulations.

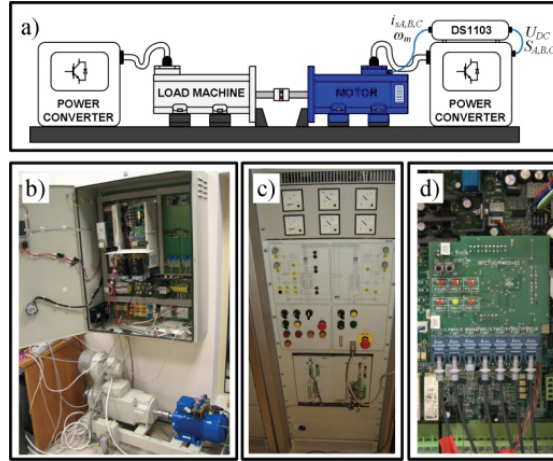


Fig. 6. The laboratory motor drive system: schematic diagram (a), photo of the induction motor drive (b) the power converter that supplies the DC motor (c) the fibre-optic modules of the inverter (d)

4.2. Validation of the diagnostic method robustness against false alarms

Figure 7 shows the time domain waveforms of the angular speed, currents, electromagnetic torque and diagnostic signal for the healthy motor drive operations that take into account various speed and load variations.

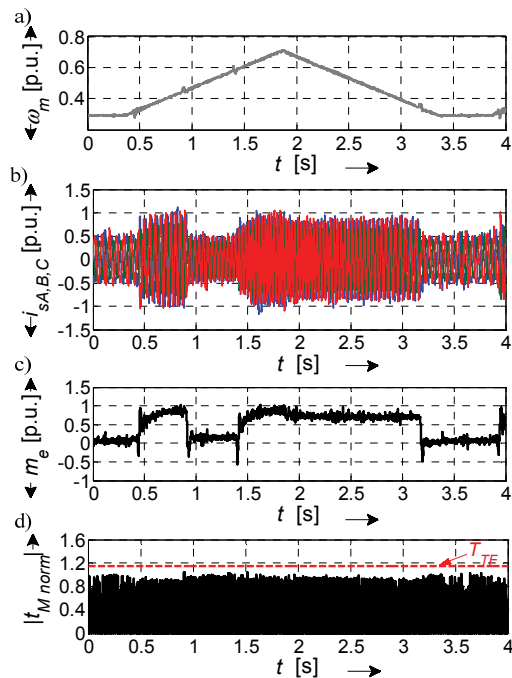


Fig. 7. Time domain waveforms achieved during the test of the diagnostic method robustness against false alarms

At the instant $t = 0.45$ s the motor was loaded when the speed of the drive was increasing. Then, at $t = 0.9$ s the load was changed from the nominal value to zero. At $t = 1.4$ s the load torque was applied $m_l = m_N$ and then at $t = 3.2$ s the load was reduced under the motor speed deceleration. In Figure 6e it is visible that the diagnostic signal does not exceed the fault threshold $T_{TF} = 1.15$ (similarly like in the simulation tests – Fig. 3), so it is justified to assume that this threshold is reached only for the faulty mode of the inverter.

4.3. Evaluation of the diagnostic method under constant speed operation of the DRFOC drive

In the LHS column of Fig. 8 experimental results obtained for the $T1$ fault, which occurred at the instant $t = 0.506$ s, under the transistor conducting mode, when the current of the faulty inverter phase i_{sA} achieved the peak value, are presented.

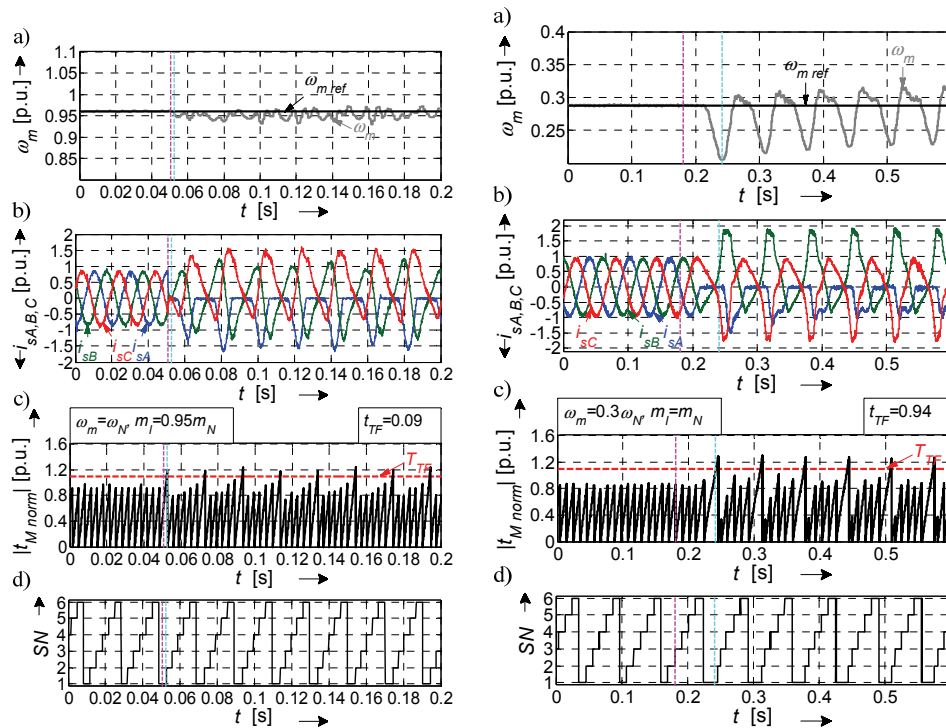


Fig. 8. Reference $\omega_{m\text{ref}}$ and measured ω_m angular motor speed (a), phase currents $i_{sA, B, C}$ (b), the diagnostic variable $|t_{M\text{norm}}|$ (c) and SN signal (d) during $T1$ open-circuit fault, for the motor drive operation under: LHS – nominal reference angular speed $\omega_{m\text{ref}} = \omega_N$ and the load torque $m_l = 0.95m_N$; RHS – reference angular speed $\omega_{m\text{ref}} = 0.3\omega_N$ and the load torque $m_l = m_N$

As can be seen in the LHS of Fig. 8(c, d), for the $SN = 1$, at $t = 0.524$ s the diagnostic signal achieved the fault threshold, so the fault localization time comprises 0.09 of the current fundamental period. Compared to the previously considered case, in the RHS of Fig. 8 results achieved for the $T1$ failure, which occurred at the instant $t = 0.181$ s, under the transistor non-

conducting mode, when the current of the faulty inverter phase i_{sA} crosses the zero-level, are shown. As is clearly seen in the RHS of Fig. 8(c, d), for the $SN = 1$, at $t = 0.241$ s the diagnostic signal reached the fault threshold, so the fault localization time comprises 0.94 of the current fundamental period.

The second considered group of transistor faults are single phase open-circuit failures. Fig. 9 presents the results which concern $T1$ and $T4$ faults, that occurred at $t = 0.162$ s, when the no-loaded motor operated at a nominal speed. At $t = 0.191$ s the diagnostic signal reached the fault threshold (Fig. 9c) when the reference voltage vector was located in the 4th sector of the α - β plane (see Fig. 9d), so the failure of $T4$ was recognized. After that, at $t = 0.234$ s the fault of $T1$ was detected. As it is visible in Fig. 9c, the failure diagnostic time is shorter than one period of the stator current fundamental harmonic, in both cases.

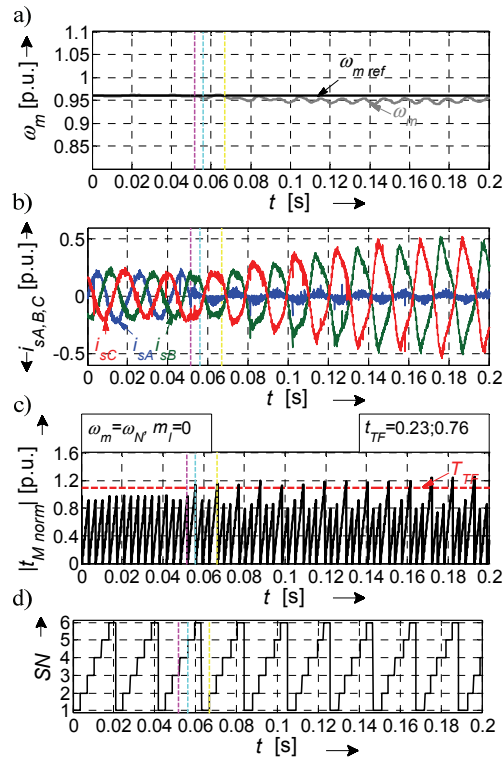


Fig. 9. Reference $\omega_{m \text{ ref}}$ and measured ω_m angular motor speed (a), phase currents $i_{sA, B, C}$ (b), the diagnostic variable $|t_{M \text{ norm}}|$ (c) and SN signal (d) during $T1$ and $T4$ open-circuit faults, for the no-loaded motor drive operation with nominal reference angular speed $\omega_{m \text{ ref}} = \omega_N$

The presented results proved the effectiveness of the proposed transistor fault diagnostic method in various motor drive conditions. Without regard to the fault instant, the transistor failure is localized faster than one period of the stator current fundamental harmonic. Additionally, thanks to diagnostic signal normalization, false alarms or a false diagnosis are avoided.

4.4. Evaluation of the diagnostic method under DRFOC drive operation at linear speed changes

In this subsection, the experimental results related to the transistor failures which occurred during linear changes of the drive speed are presented. In the LHS of the Fig. 10, the behaviour of the drive system under a single transistor fault is presented. In Fig. 10a (LHS) it is visible that at the instant $t = 0.042$ s the fault of $T1$ was introduced, when the speed of the no-loaded motor was decreased. Shortly after the fault occurrence, the diagnostic variable obtained the failure threshold at $t = 0.045$ s (see Fig. 10c). In this case, the normalized fault localization time $t_{TF} = 0.2$ is also shorter than one current fundamental period.

Next in the RHS of Fig. 10, the experimental results that concern the transistor faults in phase A of the inverter during speed increasing at 80% of nominal load torque are demonstrated. At $t = 0.146$ s the transistors $T4$ and $T1$ (phase A) failures were introduced, while the speed of the drive was increased. First, at $t = 0.157$ s the failure of $T4$ was detected and after that, at the instant $t = 0.173$ s, the $T1$ failure was localized. Similarly to the previously described experimental tests, the normalized fault localization time is shorter than one current fundamental period, in both cases ($t_{TF}(T4) = 0.35$, $t_{TF}(T1) = 0.86$).

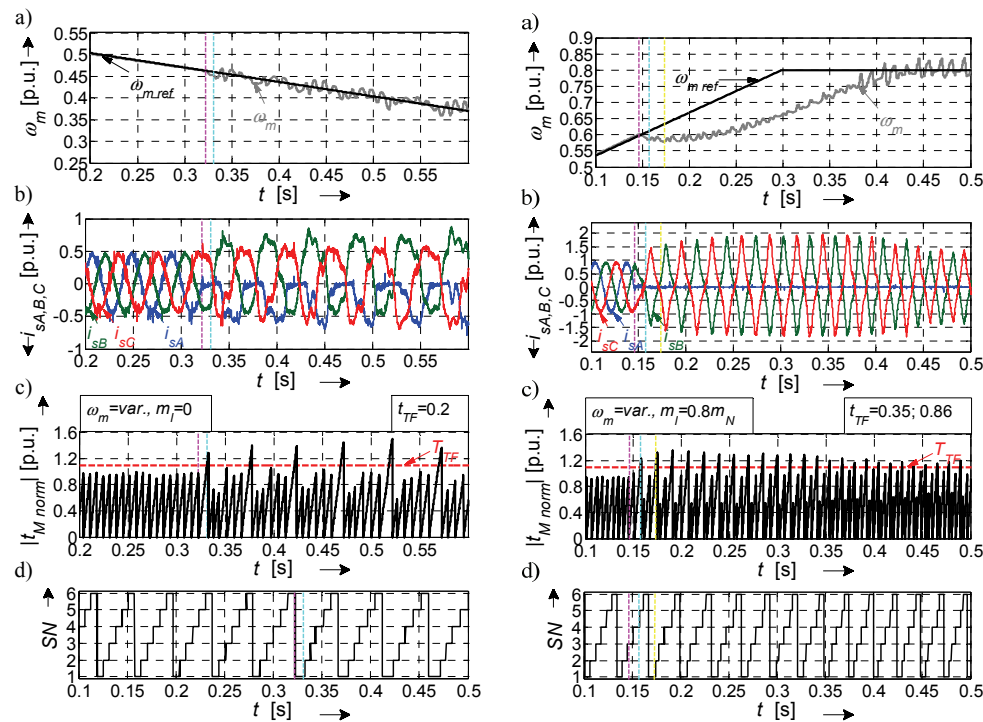


Fig. 10. Reference $\omega_{m,ref}$ and measured ω_m angular motor speed (a), phase currents $i_{SA, B, C}$ (b), the diagnostic variable $|t_{M, norm}|$ (c) and SN signal (d); LHS – during $T1$ open-circuit fault, for no-loaded motor drive operation with decreasing rotor speed; RHS – during $T1$ and $T4$ open-circuit faults, for the motor drive operation with increasing speed and the load torque $m_l = 0.8m_N$

The obtained results proved the high effectiveness of the proposed diagnostic system under various load and speed operation conditions of the motor drive. The system ensures the correct failure localization within time shorter than one period of the stator current fundamental harmonic, without regard to an instant of the fault occurrence. Additionally, this method is not limited to the detection and localization of single switch open-circuit faults only, but also ensures the detection and localization of single-phase failures.

5. Conclusions

The low-computational diagnostic method of the single switch or single phase open-circuit faults in the two-level inverter fed IM drive system is proposed in this paper. The authors have already verified the diagnostic algorithm by some simulations in the previous work, but in this paper not only new simulation research results but also the detail experimental validation of the method was presented. Additionally, the scheme of the diagnostic system was significantly simplified, which makes the approach more applicable. The proposed diagnostic technique ensures the correct single-switch open-circuit faults diagnosis as well as single-phase failures detection in a time shorter than one period of the stator current fundamental harmonic without regard to an instant of the fault occurrence and the drive operation point. The presented method gives very good results as well for constant speed operation as for variable speed of the drive system, under constant and variable load torque (including its step changes). It has been proved in simulations and laboratory experiments that the proposed method does not produce false alarms. The proposed method can be applied in all control structures of IM drives, where the information on the reference stator voltage position is known, like in DRFOC or DTC methods with SV-PWM. It is possible to extend this technique to other control strategies such as vector control with hysteresis current controllers and sinusoidal PWM, however in the case of these techniques the stator voltage vector magnitude and position have to be estimated based on the measured DC-bus voltage of the inverter.

The presented solution requires a low-computational effort and is easy applicable in modern electrical drives. The hardware implementation of the proposed transistor fault diagnostic technique can be based on a simple microprocessor system or FPGA.

Appendix

Table 2. Data of the tested induction motor drive

Quantity	Symbol	Physical units	Per unit system
power	P_N	2.2 kW	0.71
torque	m_N	14.6 Nm	0.74
speed	n_N	1440 rpm	0.96
voltage	u_N	400 V	0.71
current	i_N	4.5 A	0.71

Per unit system values have been calculated according to [2].

Acknowledgements

This work was supported by the National Science Centre (Poland) under Project 2013/09/B/ST7/04199 (2014-2017) and partially by the statutory funds of the Department of Electrical Machines, Drives and Measurements, Wrocław University of Science and Technology (2015-2016).

References

- [1] Holtz J., *Sensorless control of induction motors*, Proceedings IEEE, vol. 90, no. 8, pp. 1358-1394 (2002).
- [2] Orłowska-Kowalska T., *Sensorless induction motor drives*, Wrocław University of Technology Press (2003).
- [3] Isermann R., *Fault-Diagnosis Applications: An Introduction from Fault Detection to Fault Tolerance*, Springer Science & Business Media (2006).
- [4] Dybkowski M., Klimkowski K., Orłowska-Kowalska T., *Speed sensor fault tolerant direct torque control of induction motor drive*, 16th Inter. Power Electronics and Motion Control Conference and Exposition, PEMC 2014, Antalya, Turkey, pp. 810-815 (2014).
- [5] Romero M.E., Seron M.M., De Dona J.A., *Sensor fault-tolerant vector control of induction motors*, IET Control Theory Applications, vol. 4, no. 9, pp. 1707-1724 (2010).
- [6] Welchko B.A., Lipo T.A., Jahns T.M., Schulz S.E., *Fault tolerant three-phase ac motor drive topologies: a comparison of features, cost, and limitations* IEEE Trans. Power Electronics, vol. 19, no. 4, pp. 1108-1116 (2004).
- [7] Zhang W., Xu D., Enjeti P.N. et al., *Survey on Fault-Tolerant Techniques for Power Electronic Converters*, IEEE Trans. Power Electronics, vol. 29, no. 12, pp. 6319-6331 (2014).
- [8] Yeh C.C., Demerdash N.A.O., *Induction Motor-Drive Systems with Fault Tolerant Inverter-Motor Capabilities*, IEEE International Electric Machines and Drives Conference, IEMDC 2007, Antalya, Turkey, pp. 1451-1458 (2007).
- [9] Lu B., Sharma S.K., *A literature review of IGBT fault Diagnostic and protection methods for power inverters*, IEEE Trans. Industry Applications, vol. 45, no. 5, pp. 1770-1777 (2009).
- [10] Estima J.O. and Cardoso A.J.M., *Fast fault detection, isolation and reconfiguration in fault-tolerant permanent magnet synchronous motor drives*, Energy Convers. Congress and Exposition, Raleigh, North Carolina, USA, pp. 3617-3624 (2012).
- [11] Choi U., Lee K.B., Blaabjerg F., *Diagnosis and Tolerant Strategy of an Open-Switch Fault for T-Type Three-Level Inverter Systems*, IEEE Trans. Industry Applic., vol. 50, no. 1, pp. 495-508 (2014).
- [12] Tabbache B., Kheloui A., Benbouzid M.E.H. et al., *Research on fault analysis and fault-tolerant control of EV/HEV powertrain*, Int. Conf. on Green Energy, Sfax, Tunisia, pp. 284-289 (2014).
- [13] Sleszynski W., Nieznanski J., Cichowski A., *Open-Transistor Fault Diagnostics in Voltage-Source Inverters by Analysing the Load Currents*, IEEE Trans. Industrial Electronics, vol. 56, no. 11, pp. 4681-4688 (2009).
- [14] An Q-T., Sun L., Sun L-Z., *Current Residual Vector-Based Open-Switch Fault Diagnosis of Inverters in PMSM Drive Systems*, IEEE Trans. Power Electronics, vol. 30, no. 5, pp. 2814-2827 (2015).
- [15] Estima J.O., Marques Cardoso A.J., *A New Algorithm for Real-Time Multiple Open-Circuit Fault Diagnosis in Voltage-Fed PWM Motor Drives by the Reference Current Errors*, IEEE Trans. Industrial Electronics, vol. 60, no. 8, pp. 3496-3505 (2013).
- [16] Sobanski P., *Fuzzy-logic-based approach to voltage inverter fault diagnosis in induction motor drive*, Przegląd Elektrotechniczny, vol. 90, no. 6, pp. 149-153 (2014).
- [17] Orłowska-Kowalska T., Sobanski P., *Simple Sensorless Diagnosis Method for Open-Switch Faults in SVM-VSI-fed Induction Motor Drive*, IEEE 39th Ann. Conf. Industrial Electronics Society IECON'2013, Vienna, Austria, pp. 8210-8215 (2013).
- [18] Sobanski P., Orłowska-Kowalska T., Kowalski C.T., *Multiple transistor open-circuit faults diagnosis in a vector-controlled induction motor drive*, IEEE Intern. Conf. on Industrial Technology ICIT'2015, Seville, Spain, pp. 3238-3242 (2015).

-
- [19] Espinoza-Trejo D.R., Campos-Delgado D.U., Bossio G. et al., *Fault diagnosis scheme for open-circuit faults in field-oriented control induction motor drives*, IET Power Electronics, vol. 6, no. 5, pp. 869-877 (2013).
 - [20] Alavi M., Wang D., Luo M., *Short-Circuit Fault Diagnosis for Three-Phase Inverters Based on Voltage-Space Patterns*, IEEE Trans. on Industrial Electronics, vol. 61, no. 5, pp. 5558-5569 (2014).
 - [21] Alavi M., Luo M., Wang D., Bai H., *IGBT fault detection for three phase motor drives using neural networks*, 17th Conf. on Emerging Technol. and Factory Automation, Krakow, Poland, pp. 1-8 (2012).